

## Article

# Recycled Carbon Nanofiber-Polypropylene Nanocomposite: A Step towards Sustainable Structural Material Development

Abhishek Kumar Pathak \* and Tomohiro Yokozeki

Department of Aeronautics and Astronautics, The University of Tokyo, Tokyo 113-8656, Japan

\* Correspondence: abhishek.pathak@aastr.t.u-tokyo.ac.jp

**Abstract:** Plastic products play a significant role in fulfilling daily necessities, but the non-decomposable nature of plastic leads to inescapable environmental damage. Recycling plastic material is the most appropriate solution to avoid pollution and short product lifespan. The present study shows the recycling effect on carbon nanofiber (CNF) reinforced polypropylene (PP) nanocomposite to attain the purpose of reuse and sustainability. 30 wt% CNF melt-blended with polymer and PP-nanocomposites were fabricated using the injection molding technique. PP-CNF nanocomposites were recycled, and mechanical, thermal, and morphological properties were investigated. Three-point bending and tensile testing showed a low decrement of ~1% and ~5% in bending and tensile strength after recycling 30 wt% PP-CNF nanocomposites. Scanning electron microscopy (SEM) images show that the alignment of CNF was disturbed after recycling due to the decrement in the aspect ratio of CNF. Differential scanning calorimetry (DSC) and X-ray diffraction (XRD) showed that the crystallinity of PP increases with recycling. The lowering of interfacial interaction between CNF and PP after recycling was studied by a stress-controlled rheometer. The decrement in mechanical properties of PP-CNF nanocomposite is not significant due to CNF reinforcement; hence, it can be reused for the same or other structural applications.



**Citation:** Pathak, A.K.; Yokozeki, T. Recycled Carbon Nanofiber-Polypropylene Nanocomposite: A Step towards Sustainable Structural Material Development. *J. Compos. Sci.* **2022**, *6*, 332. <https://doi.org/10.3390/jcs6110332>

Academic Editor: Francesco Tornabene

Received: 22 September 2022

Accepted: 1 November 2022

Published: 3 November 2022

**Publisher's Note:** MDPI stays neutral with regard to jurisdictional claims in published maps and institutional affiliations.



**Copyright:** © 2022 by the authors. Licensee MDPI, Basel, Switzerland. This article is an open access article distributed under the terms and conditions of the Creative Commons Attribution (CC BY) license (<https://creativecommons.org/licenses/by/4.0/>).

**Keywords:** recycling; carbon nanofiber (CNF); mechanical properties; thermal stability; rheology; interfacial interaction

## 1. Introduction

Plastic materials are widely used in packaging, electronics, construction, daily household, automobiles, and aerospace industries due to their versatility, low cost, and high strength-to-weight ratio. Most plastic materials are non-degradable, producing a very high content of waste material and badly influencing the environment [1]. One study by Laurent estimated that between 60–99 million metric tonnes (Mt) of mismanaged plastic waste was produced globally in 2015. In a business-as-usual scenario, this figure could triple to 155–265 Mt  $y^{-1}$  by 2060 [2]. The third component of the modern waste management rule, i.e., recycling, is a crucial solution for non-degradable plastic materials. One significant benefit of the recycling process is substantial economic remunerations obtained by replacing high-cost virgin materials with recycled materials. In typical industrial practice, virgin thermoplastic material is mixed with recycled waste (approx. 20%) to fabricate the new part; hence, recycling is key to reducing cost. Plastic waste is generally divided into two categories: process waste generated in the form of defective, flash parts, etc., and aged waste, which is obtained after serving the designated life of materials. In daily lifestyle tools, polypropylene (PP), low-density polyethylene (LDPE), high-density polyethylene (HDPE), polystyrene (PS), and polyvinyl chloride (PVC) are used as significant plastic materials [3]. PP is an attractive thermoplastic material due to its outstanding qualities, such as lightweight, non-toxicity, ease of processability, low production cost, and recyclable nature [4–6]. In 2018, Lopez and his team reported that polyolefins account for more than half of plastic production, and especially PP alone stands for 19% in various fields such as packaging (39.9%), building materials (19.7%), and automobile industries (8.9%) [7].

Various processes, such as extrusion, injection molding, and compression, can be used to fabricate PP products. Recycling PP via reheating and remolding introduces weakness in the product's mechanical properties [8,9]. In recent years, considerable research has been conducted to resolve the issue of plastic waste reduction by recycling. Polymer modification via polymer blending (solution blending/melt blending) is a standard method to tailor the properties of the recycled polymer. Polymers such as thermoplastic polyurethane (TPU) [10] and acrylonitrile-butadiene-styrene (ABS), with or without compatibilizer used by different research groups to improve the PP properties [11]. In a similar direction, Zaghoul studied the role of different inorganic as well as a carbon filler in different polymeric materials and showed the importance of nanofillers in improving the mechanical properties of polymeric materials [12–15]. The most common problem of these polymer blends is the recovery of interfacial properties after repeat recycling. It is a fact that after no. of recycling, the mechanical and thermal properties of the polymer blend deteriorated significantly, and consequently, blending is not a successful technique for multiple recycling.

Few studies have been reported on natural fiber-reinforced thermoplastic and its recycling effect on the mechanical performance of natural fiber-reinforced nanocomposites. Few researchers have reported the effect of bagasse fiber reinforcement on polyethylene [16], polypropylene [17], and polyethylene terephthalate (PET) [18] and reported the improvement in tensile properties. Bourmaud and Baley studied the role of hemp and sisal on recycled polypropylene and showed that the tensile modulus could be conserved after recycling [19]. One of the significant issues with natural fiber-reinforced thermoplastic after recycling is the considerable variation in properties of the natural fiber after thermal recycling, which results in a significant difference in mechanical properties, and it is not ideal for structural application.

In this direction, carbon nanomaterials play a very vital role because of their high thermal stability. Carbon nanofiber (CNF) is a high strength reinforcement that can be used as a polymer modifier. The intrinsic properties of CNF are expected to be unaffected after multiple recycling due to high thermal stability (more than 1000 °C) [20,21].

The feasibility of reprocessing CNF-reinforced PP composites has not been investigated appropriately yet. Therefore, composites made from recycled CNF and PP are not being used in industries with their full potential. The present work aims to examine the effect of recycling on the mechanical and thermal performance of CNF-reinforced PP nanocomposites using the extrusion and injection molding process. The variation of mechanical and thermal properties of recycled PP-CNF nanocomposite is explained based on changes in the aspect ratio of CNF, crystallinity, and interfacial interaction behavior. The effect of recycling on the tensile and flexural behavior of nanocomposites has been studied. Interfacial and thermal properties of recycled PP-CNF nanocomposites are studied by stress-controlled Rheometer, differential scanning calorimetry (DSC), and thermogravimetric analysis (TGA). The scanning electron microscope (SEM) and the optical microscope have been used to study the fractured surface of nanocomposites. The crystallinity of the nanocomposites has been studied by X-ray diffraction (XRD).

## 2. Materials and Methods

### 2.1. Materials

The high-strength PP (homopolymer with tensile strength and modulus 35 MPa and 1.65 GPa) was procured from ALMEDIO INC., Tokyo, Japan. Commercial produces high-modulus crystallized CNF with an average diameter of 0.2–0.8  $\mu\text{m}$ , grain size 1–15  $\mu\text{m}$  (D50) was procured from ALMEDIO INC., Tokyo, Japan.

### 2.2. Fabrication of PP-CNF Composite

The PP was separately mixed with CNF (30 wt% content) in the bi-axial kneading extruder. The blending occurred at 200 °C with a screw diameter of 25 mm with 61 ratios of length/diameter (L/D) in the melting section. 30 wt% CNF was mixed with PP, and CNF-PP nanocomposites (PP-CNF-1) were fabricated using injection molding at 200 °C. During

the CNF-PP nanocomposite fabrication, no sizing agent was used for CNF dispersion in PP. In the second round, PP-CNF nanocomposite was recycled using a bi-axial kneading extruder, and new PP-CNF palates were obtained. 1st recycled PP-CNF nanocomposites (PP-CNF-2) were fabricated using injection molding under the same manufacturing conditions as PP-CNF-1. Similarly, second recycled PP-CNF nanocomposites (PP-CNF-3) were obtained following the same procedure as PP-CNF-2. In this study, five samples of each composition are used to evaluate the mechanical and thermal properties of nanocomposites. The list of the three types of fabricated samples is shown in Table 1. During the fabrication, no manufacturing defect was detected, and for evidence, sample images and optical images of their fractured surface are shown in Figure 1.

**Table 1.** List and description of the nanocomposite specimens.

Sample Designation	Details	CNF Content (wt%)
PP-CNF-1	Pure PP with CNF	30
PP-CNF-2	1st Recycled PP with CNF	30
PP-CNF-3	2nd Recycled PP with CNF	30

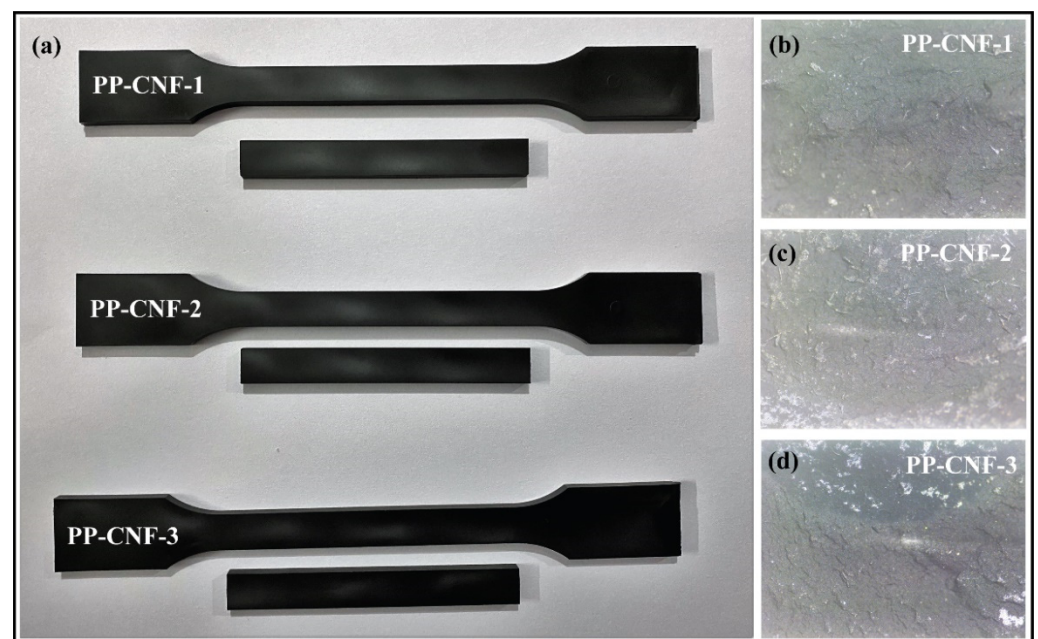


**Figure 1.** (a) Digital image of PP-CNF nanocomposite samples prepared for bending and tensile testing shows no manufacturing defect, and optical images of fractured cross-section show the defect-free surface of (b) PP-CNF-1, (c) PP-CNF-2, and (d) PP-CNF-3.

### 2.3. Characterization Methods

The mechanical properties of three different CNF-PP nanocomposites were measured by Instron Universal Testing Machine (UTM) 5582. Three-point bending test was conducted according to the ASTM D790-17 standard. The bending strength was measured on the sample of a length of 80 mm, a width of 10 mm, and a thickness of 4 mm by a three-point bending test at a cross-head speed of 1 mm/min. The tensile strength of dog bone-shaped PP-CNF nanocomposites was conducted according to the ASTM D638 standard. A dog bone type 1 sample with 4 mm thickness and 10 mm width was used for the testing. All the tests were performed at 2 mm/min using an extensometer of a fixed length of 25 mm. Shore D hardness test was conducted using a Tekcoplus Shore D durometer following ASTM standard D2240. The test was conducted with a needle length of 2.5 mm using a

measuring power of 44.5 N. Five specimens were tested for tensile, bending, and hardness mechanical testing for each composition.

The melting and recrystallization temperature of PP-CNF palates were calculated using DSC (Shimadzu, Tokyo, Japan) in the nitrogen atmosphere (flow rate 100 mL/min) at the temperature range 25–250 °C with a temperature rate of 3 °C/min. The change in crystallinity behavior after the recycling of PP was studied by XRD (D-8 Advanced Bruker powder X-ray diffractometer) using CuK $\alpha$  radiation ( $\lambda = 1.5418 \text{ \AA}$ ) at a scanning rate of 2°/min with a voltage of 40 kV with a current of 40 mA within range of  $2\theta = 5\text{--}60^\circ$ . The thermal stability of PP-CNF nanocomposites was analyzed by TGA (DTA-60, Shimadzu, Japan) in the nitrogen atmosphere with a 50 mL/min flow rate and 10 °C/min temperature rate. Maximum thermal degradation temperature ( $T_d$ ) was recorded by differential thermal analysis (DTA). The surface morphology of fractured PP-CNF nanocomposites and the average aspect ratio of CNF were recorded by desktop SEM Hitachi miniscope (TM4000 plus).

The viscoelastic properties of recycled PP nanocomposite were examined by a stress-controlled Rheometer (Rheoplus MCR52 SN81442416, Delhi, India) at a fixed temperature of 200 °C equipped with 25 mm parallel plate geometry. In the linear viscoelastic regime, small amplitude oscillatory shear (SAOS) frequency sweep tests were performed in the range of 0.1–100 rad/s. The intermolecular interaction between CNF and PP was measured by Fourier transform infrared (FT-IR) in ATR mode.

### 3. Results and Discussion

#### 3.1. Mechanical Properties Analysis

The mechanical properties of CNF-reinforced PP nanocomposite samples are initially investigated by a 3-point bending test and displayed in Figure 2. It is observed that the mechanical performance of PP polymer is highly dependent on the type and ratio of reinforcement used [4]. In the case of PP-CNF-1, the maximum flexural strength of 95.5 MPa is registered, while in the case of PP-CNF-2, slightly lower flexural strength (95.4 MPa) is observed due to the first recycling. In the case of PP-CNF-3, the flexural strength of 94.2 MPa is registered, which is the lowest (Figure 2a).

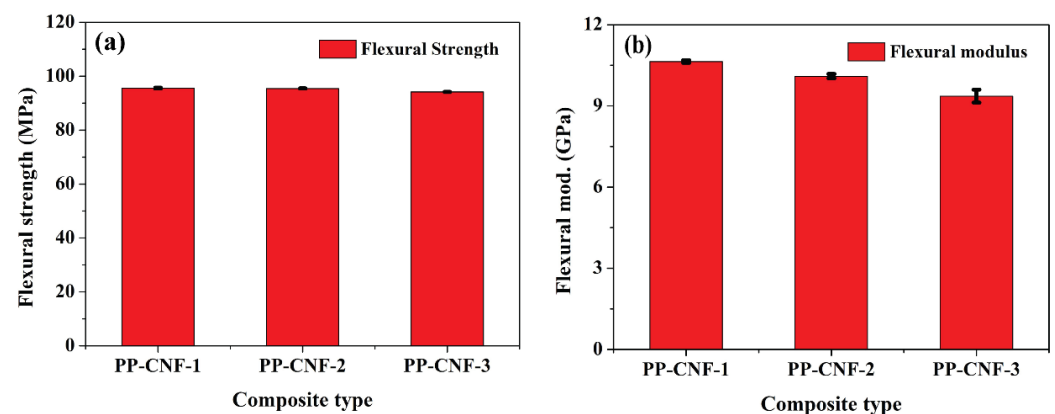


**Figure 2.** Three-point bending testing results of PP-CNF nanocomposite according to ASTM D790 standard and showed the plot of (a) Flexural strength and (b) Flexural modulus variation of PP-CNF nanocomposite.

A similar trend of curve behavior is observed for the flexural modulus of PP-CNF nanocomposites (Figure 2b). It is observed that with no. of recycling of nanocomposite, the flexural modulus decreases. The calculated flexural modulus of PP-CNF-1, PP-CNF-2, and PP-CNF-3 is 10.6, 10.1, and 9.3 GPa, respectively. This result shows that recycling affects the mechanical performance of polymer nanocomposites [22]. With an increment in recycling, a decrement in the bending strength and modulus of the nanocomposite is observed. The

bending properties decrease insignificantly because CNF reinforcement helps bind the polymer together even after recycling.

The fracture behavior and extension in nanocomposite before break can be seen in the Stress-Strain curve, shown in Figure 3. All the nanocomposites show brittle fracture behavior, and the stiffness of nanocomposites decreases with an increment in the recycling of PP nanocomposites (Figure 3a–c). It is because of polymer chain break during the recycling, which lowers the extent of cross-linking in PP. Hence, the maximum strain is observed for second recycled PP nanocomposites (PP-CNF-3). The effect of recycling is also detected in the maximum load-bearing capacity curve, and the maximum load is sustained by PP-CNF-1 (Figure 3d). Even after recycling, low decrement in the mechanical performance of PP-CNF nanocomposites is due to strong interfacial adhesion because of CNF alignment and its surface roughness [4].

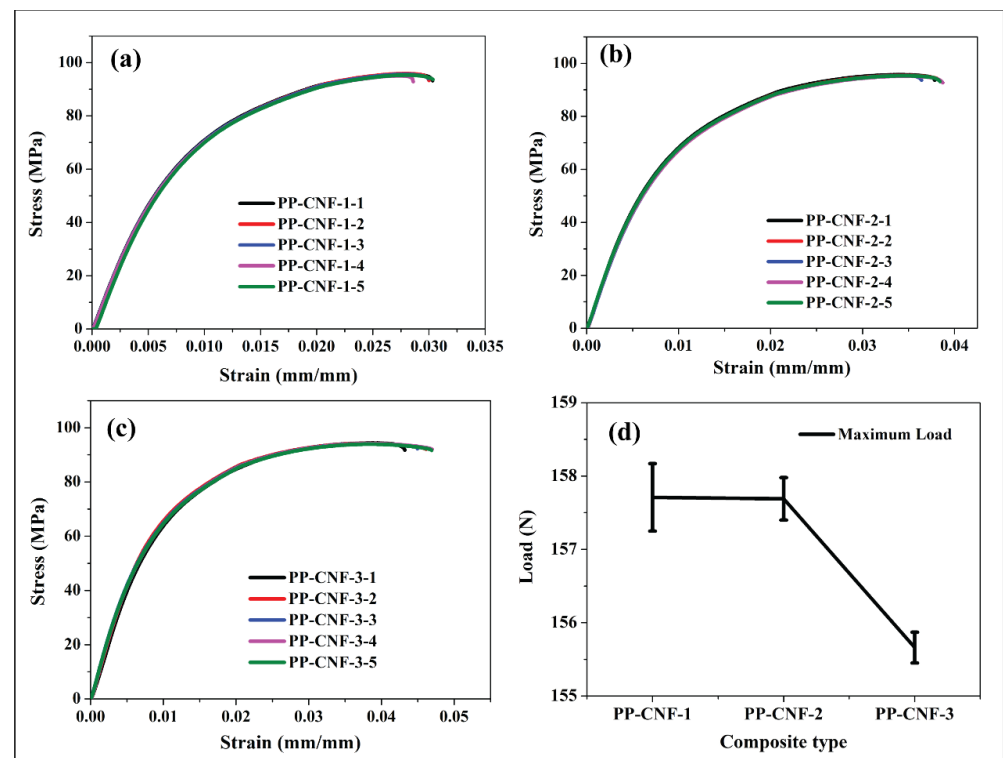


**Figure 3.** Stress-strain curve of (a) PP-CNF-1, (b) PP-CNF-2, (c) PP-CNF-3, and (d) Maximum load variation with different composite type.

The tensile strength variation of the PP nanocomposite is shown in Figure 4. The tensile setup used for testing is shown in Figure 4a. It is observed that the tensile strength of PP-CNF nanocomposite decreases as we increase the no. of recycling. For PP-CNF-1 nanocomposite, a tensile strength of 53.9 MPa is registered, while the tensile strength value decreased to 52.3 and 51.0 MPa for PP-CNF-2 and PP-CNF-3, respectively (Figure 4b).

The tensile modulus is calculated by the stress-strain curve and displayed in Figure 4c. The same trend is observed in the tensile modulus, where the maximum modulus is reported for PP-CNF-1 (Figure 4c). As we can see, the contribution of CNF to the improvement of mechanical properties is very significant, and the difference in modulus after recycling is not very high. For PP-CNF-1, 11.9 GPa of modulus is registered, while in the case of PP-CNF-2 and PP-CNF-3, it decreased to 10.9 and 10.2 GPa, respectively. The lowering of mechanical properties is due to the weakening of interfacial interaction between PP nanocomposite after recycling, which can be reflected in the stress-strain curve and displayed in Figure 5.

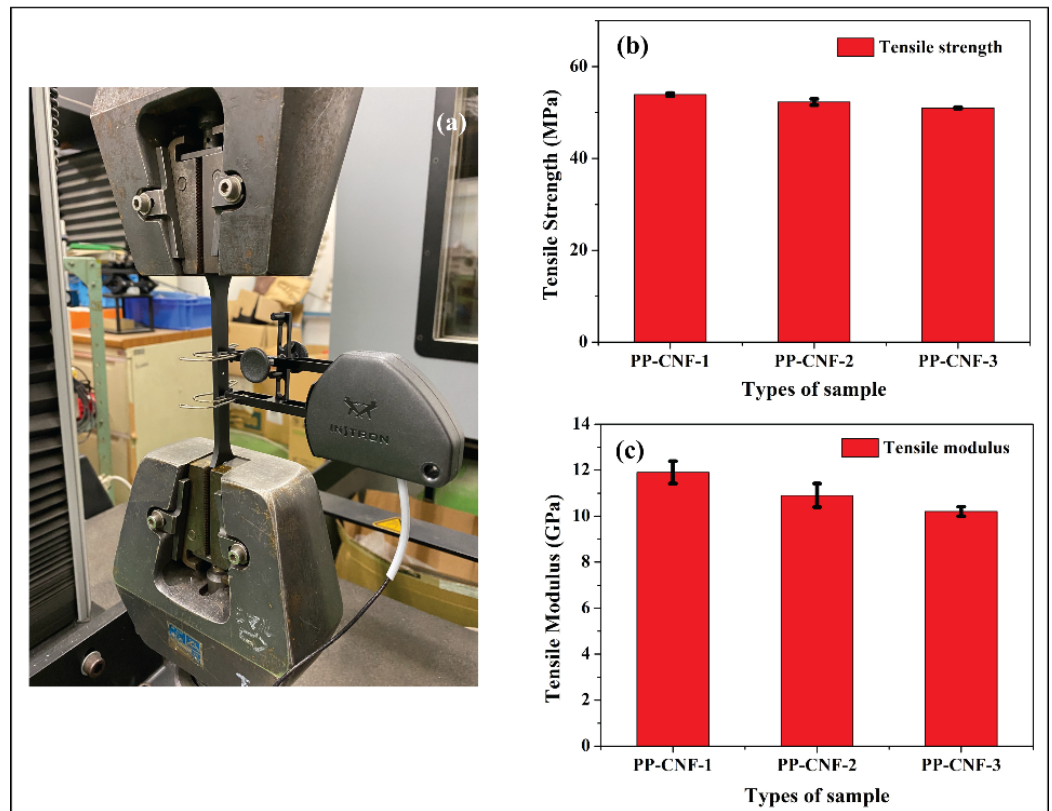


**Figure 4.** (a) Tensile testing setup with extensometer for PP nanocomposite as per ASTM D638, (b) Tensile strength is recorded at ultimate strength point, and (c) Stress-strain curve shown by the extensometer calculates tensile modulus.

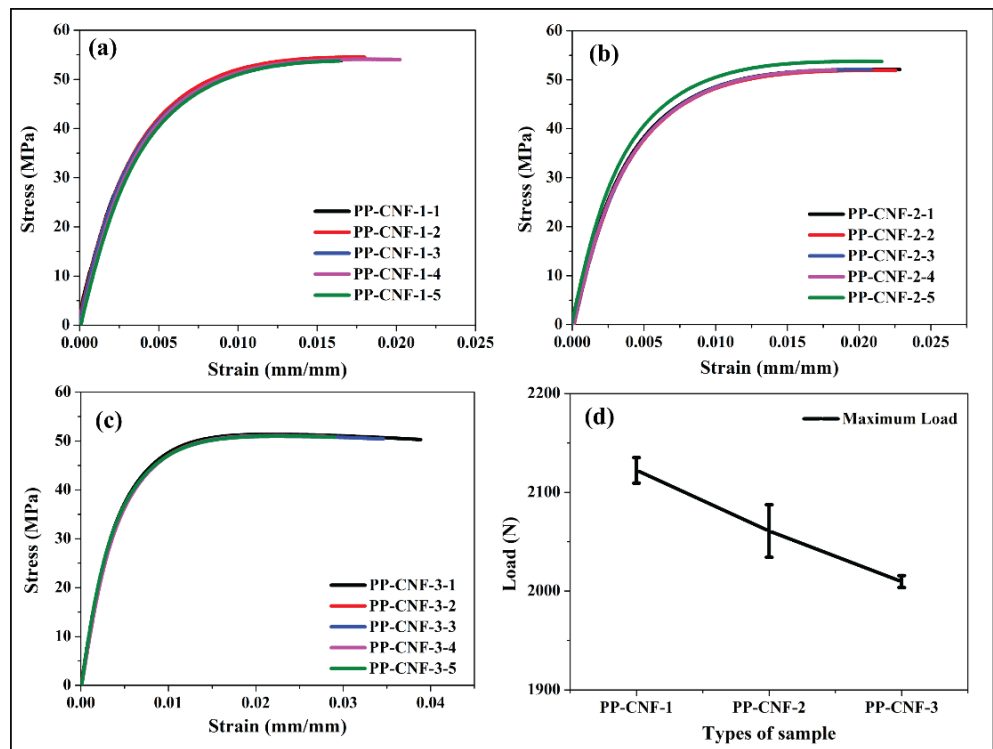


**Figure 5.** Stress-strain curve of (a) PP-CNF-1, (b) PP-CNF-2, (c) PP-CNF-3, and (d) Maximum tensile load variation with different PP nanocomposites.

In Figure 5a–c, the effect of recycling on the stiffness of the material can be clearly seen. With recycling, nanocomposite possesses an increase in strain, which indicates a weakening in the bonding of PP after recycling. Consequently, the tensile load-bearing tendency decreases with the increment of recycling (Figure 5d). The low difference in load-bearing capacity of CNF-reinforced PP nanocomposites after recycling is because of CNF intrinsic properties and strong interfacial interaction [23,24]. With all the above data, we can predict that the CNF can be used as efficient nanofillers for recycled polymer.

In CNF-reinforced nanocomposite, the mechanical properties are explained by its structure and alignment, which is similar to truncated conical stacks of graphene and affects the load transfer capacity due to inhibition of lateral sliding of graphene sheets in polymer nanocomposites [25].

### 3.2. Morphological Study by SEM

SEM observation of the fractured surface of PP nanocomposites filled with CNF is shown in Figure 6. In Figure 6a,c,e, the fractured surface of the nanocomposite is displayed. In Figure 6b,d,f, the morphology of CNF is shown after separating them from polymer to study the average aspect ratio of CNF after recycling. The mechanical properties of PP-CNF nanocomposites mainly depend on the dispersion and alignment of CNF in PP. In Figure 6a,b, SEM images of fractured PP-CNF-1 surfaces at different magnifications are displayed. It is observed that the CNF is very well dispersed and oriented in all the nanocomposites, and very slight disorientation of fiber can be seen due to the different sizes of CNF present in the PP nanocomposite [4]. In Figure 6c,d, fractured surface of PP-CNF-2 is shown, and the orientation of CNF is also the same as PP-CNF-1. Hence, a low difference in mechanical properties is observed after the recycling of PP-CNF nanocomposites. A similar observation is seen in the SEM of PP-CNF-3 fractured surface (Figure 6e,f), and no significant changes on the fracture surface are observed. One major reason for the change in mechanical properties of PP-CNF nanocomposite after recycling is the change in the aspect ratio of CNF. It is reported that the aspect ratio of CNF is affected after recycling, and as a result, the dispersion variation can be seen in the nanocomposites. In the present case, the average aspect ratio was calculated by taking the average of 100 fibers dimensions using SEM and 11.6, 9.6, and 6.5 of the average aspect ratios of CNF in PP-CNF1-, PP-CNF-3, and PP-CNF-3 is reported, respectively. It can be inferred that the low aspect ratio of CNF in PP-CNF-3 is the reason for poor dispersion (in the form of agglomeration) and results in minimum mechanical properties [17,26].

The decrement in aspect ratio CNF significantly affects its interaction with polymer. This results in a lowering of the hardness of nanocomposites after recycling. Shore D hardness of nanocomposites is evaluated using a Durometer, and shore D hardness of  $77.5 \pm 0.35$ ,  $75.5 \pm 2.02$ , and  $74.2 \pm 3.32$  HD for PP-CNF-1, PP-CNF-2, and PP-CNF-3 is observed. The lowering of hardness signifies the importance of the aspect ratio of nanomaterials, which plays an essential role in determining mechanical properties.

### 3.3. Thermal Analysis of PP Nanocomposite

DSC of PP nanocomposites is used to see the effect of recycling on the melting and crystallization temperature of PP and is shown in Figure 7a. Two types of peaks in the heating and cooling DSC curve are observed: the endothermic peak (designated as melting temperature) and the exothermic peak (defined as crystallization temperature). It is observed that the melting temperature ( $T_m$ ) is unaffected by the recycling process, and hence the material still possesses its original properties even after the second recycling. However, some minor changes in chemical interaction happened due to the recycling process. For all the specimens,  $\sim 167$  °C melting temperature is observed. Moreover, the recycling process does not significantly affect the crystallization temperature ( $T_c$ ). All the value of  $T_m$  and  $T_c$  is shown in Table 2. In the recycling process, the crystallinity of the polymer significantly

changed, and using the DSC melting curve, the crystallinity of the polymer was evaluated. The degree of crystallinity ( $X_c$ ) is calculated by using Equation (1) [27,28].

$$X_c = \frac{\Delta H_f \times 100}{\Delta H_{100}} \quad (1)$$

where  $\Delta H_f$  is the enthalpy of fusion of specimen, and  $\Delta H_{100}$  is the enthalpy of fusion for 100% crystalline specimen (209 J/g for PP).

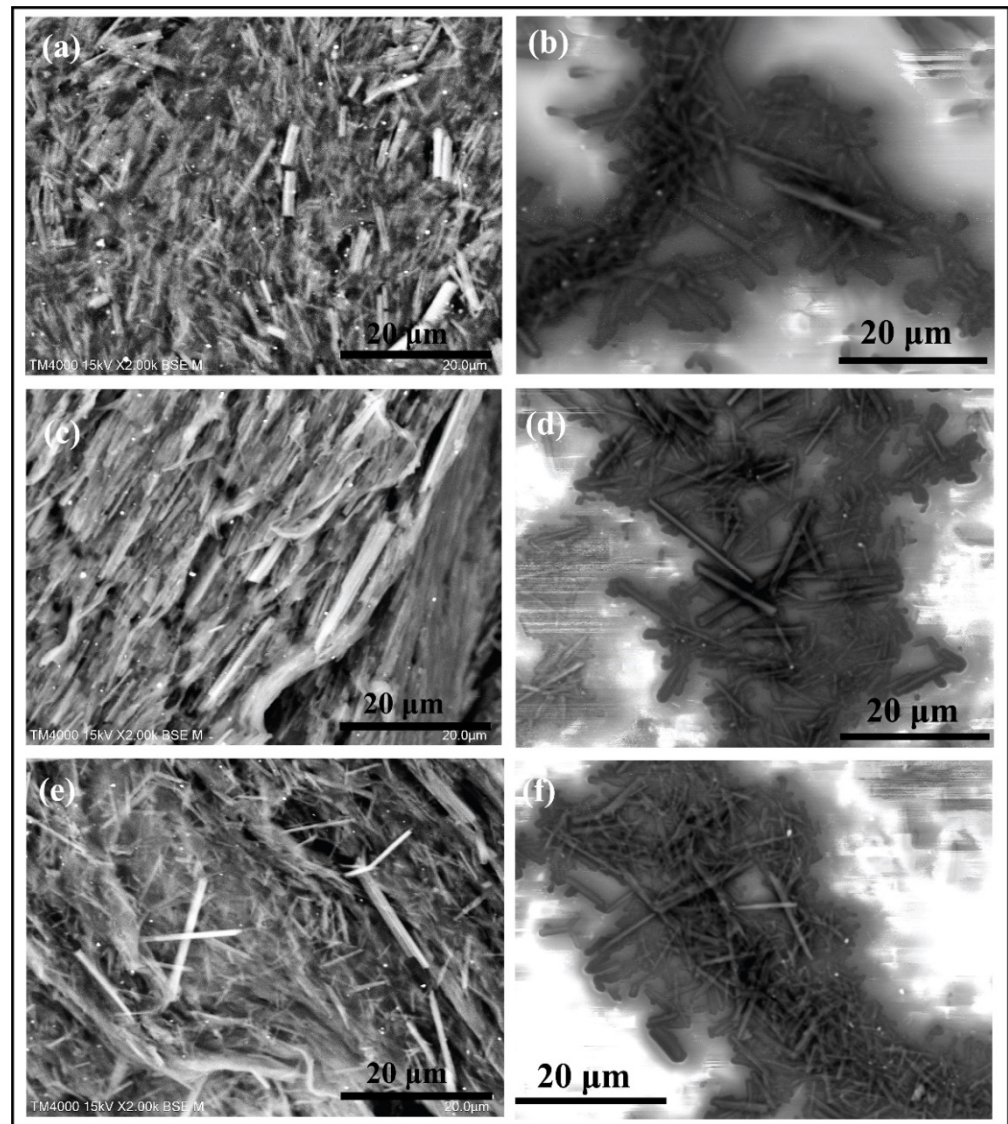


**Figure 6.** Fractured surface morphology to see the alignment of CNF and CNF surface study of (a,b) PP-CNF-1, (c,d) PP-CNF-2, and (e,f) PP-CNF-3 nanocomposites.

$\Delta H_f$  is calculated by calculating the area under of melting peak of PP (Figure 7b). It is observed that the crystallinity of PP increases after recycling. Higher crystallinity of the polymer results in its higher mechanical performance [22]. The  $X_c$  of 60.3, 61.1, and 61.3% for PP in PP-CNF-1, PP-CNF-2, and PP-CNF-3 are reported (Figure 7d). The change in the % crystallinity in polymer arises from the breaking and rearrangement of the long polymer chain after recycling [17,29]. The improvement in % crystallinity of PP is not significant hence it can be concluded that the recycling of PP is not significantly affecting PP properties. Hence the change in CNF properties is the significant reason behind the variation of mechanical properties.

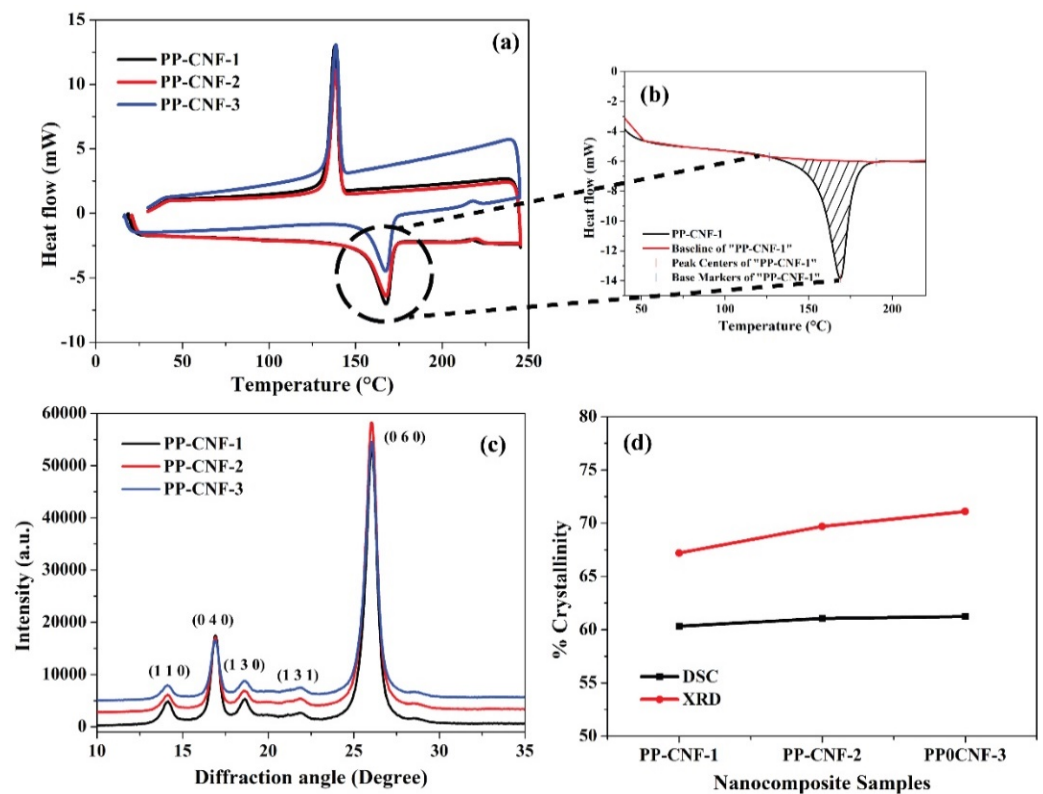


**Figure 7.** (a) Melting and recrystallization temperature by DSC, (b) % crystallinity calculation by DSC, (c) XRD study to see the crystalline plane of PP after recycling, and (d) %crystallinity comparison calculated by DSC and XRD of PP-CNF nanocomposites.

**Table 2.** Thermal properties of PP-CNF nanocomposites.

Sample Designation	T <sub>m</sub> (°C)	T <sub>c</sub> (°C)
PP-CNF-1	167.7	138.0
PP-CNF-2	167.5	138.4
PP-CNF-3	167.3	138.6

The improvement in %crystallinity of PP after recycling is confirmed by XRD analysis (Figure 7c). The Ruland-Wonk method is used to find out the crystallinity of PP after recycling using Equation (2) [17].

$$\% \text{ crystallinity} = \frac{\text{Crystalline area} \times 100}{\text{Total area of curve}} \tag{2}$$

In Figure 7c, five crystalline peaks of PP are observed around 14.2, 16.9, 18.6, 21.8, and 26.1°, designated to 110, 040, 130, 131, and 060 crystalline planes of PP. From the curve (Figure 7c), a change in the intensity of crystalline PP after recycling is seen. The calculated % crystallinity of PP in PP-CNF-1, PP-CNF-2, and PP-CNF-3 are 67.2, 69.7, and 71.1%, shown in Figure 7d.

The recycling effect on PP-CNF nanocomposite interfacial properties is studied by a stress-controlled Rheometer. In the stress-controlled rheological analysis, the maximum applied strain is fixed, and a change in viscoelastic behavior is recorded [30]. Figure 8 shows the effect of recycling on the storage modulus (*G'*) and loss modulus (*G''*) of PP-CNF nanocomposite with strain. With the increment of recycling on PP-CNF nanocomposite, *G'* and *G''* decreases (Figure 8a,b). It is also observed that the value of *G'* and *G''* decreased

with strain increment, and the decrement in modulus due to strain increment can be seen. It is because of the change in structural properties of nanocomposites [30].

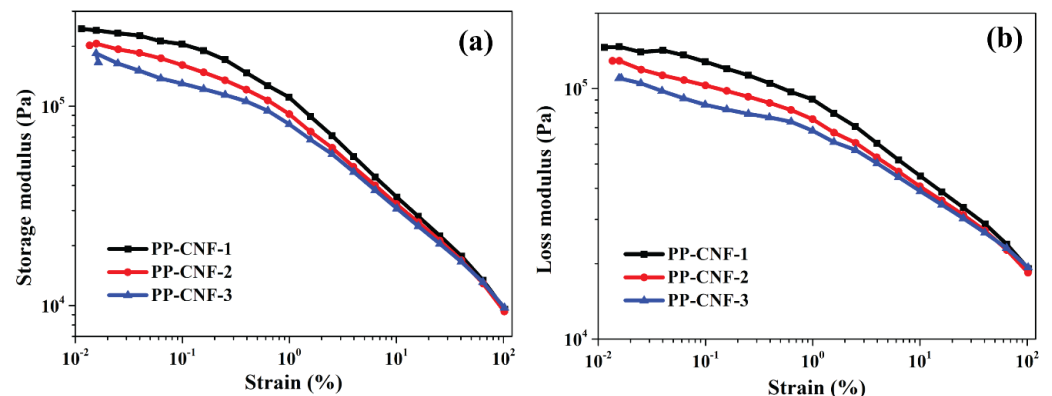


**Figure 8.** Stress-controlled Rheometer study of (a) storage modulus ( $G'$ ) and (b) loss modulus ( $G''$ ) of recycled PP-CNF nanocomposites with strain with varying no. of recycling at 200 °C.

Variation in  $G'$ ,  $G''$ , and complex viscosity ( $\eta^*$ ) of recycled PP-CNF nanocomposite with respect to angular frequency is displayed in Figure 9. At lower frequencies, the  $G'$  and  $G''$  value of PP-CNF-1 is higher, and the value of  $G'$  and  $G''$  decreases with recycling of PP-CNF nanocomposites (Figure 9a,b). It is observed that the rate of increment of  $G'$  and  $G''$  with frequency rate is almost similar (no overlapping of the curve). It signifies the similar nature of interfacial behavior in PP-CNF nanocomposite after recycling. The value of  $G'$  is more than twice of  $G''$ , which indicates the non-terminal behavior of nanocomposite [30,31]. The non-terminal behavior of PP-CNF nanocomposites at a lower frequency is due to the interconnected network between CNF and PP (interfacial interaction), and the formed interconnected network tendency decreased after recycling nanocomposites. As the reinforcement content in PP nanocomposite is very high and the same in all the specimens, CNF-CNF interaction begins to dominate, leading to an interconnected network structure. As the sample contains the same CNF,  $G''$  shows a similar trend as  $G'$  for all three types of nanocomposites, even after recycling. It is also observed that the interconnected network weakens after the recycling, and as a result,  $G'$  and  $G''$  value decrease after every recycling. All the PP-CNF nanocomposites showed viscous behavior, which is indicated by the increment in modulus value with an increment in angular frequency [32,33].

The effect of recycling on the interfacial network of PP-CNF nanocomposite can be studied by complex viscosity ( $\eta^*$ ), which is a measure of the total resistance to flow as a function of angular frequency (Figure 9c). With the increase in recycling,  $\eta^*$  decreases. At lower frequencies, the effect of CNF is noticeable and the effect of CNF at higher frequencies diminished due to shear thinning behavior (non-Newtonian nature of polymer composite). The shear-thinning behavior in PP-CNF-2 is maximum due to weak interfacial interaction between CNF and PP due to second recycling. At lower frequencies, complex viscosity is maximum for PP-CNF-1, indicating that the restrain in polymer chain relaxation due to the presence of CNF gets lower after recycling PP-CNF nanocomposite. Hence, it can be assumed that the CNF-CNF interaction is maximum in PP-CNF-1 and its interaction with PP is maximum, restraining the long-range motion of polymer chains. While, with an increment in recycling, the CNF-CNF interaction with PP decreases, and hence, lower mechanical and thermal properties, are reported [31,32].

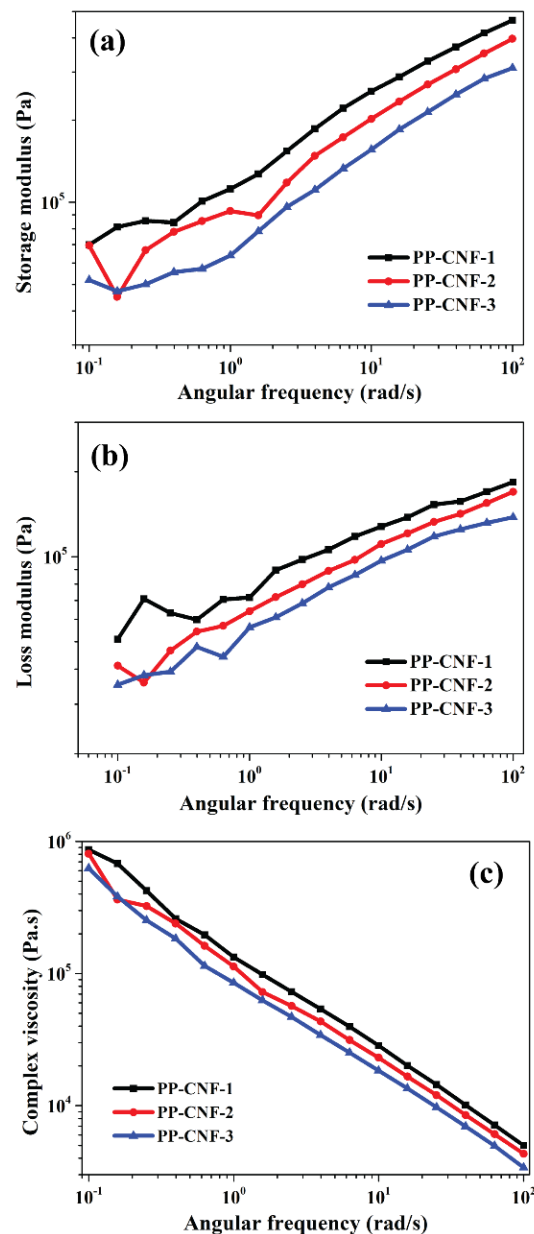


**Figure 9.** Variation of (a) storage modulus ( $G'$ ), (b) loss modulus ( $G''$ ), and (c) Complex viscosity ( $\eta^*$ ) of recycled PP-CNF nanocomposites with frequency sweep with varying no. of recycling at 200 °C.

TGA and DTA are used to find the nanocomposite's degradation and the CNF content (Figure 10). By comparing the wt% loss as a function of increasing temperature, the effect of recycling on the thermal stability of PP nanocomposite has been analyzed. In all the specimens, the approximate weight left is around 30% CNF in the nanocomposite. Hence, TGA verifies the CNF content, which is the same in all the specimens. It also inferred that CNF is thermally stable at higher temperatures, and no weight loss in CNF is observed in every sample [4]. DTA calculates thermal degradation temperature, showing two significant peaks; one is associated with the removal of volatile content from the sample, and the other is the degradation of PP polymer in the nanocomposite. The degradation temperature is not primarily affected by polymer recycling, and the degradation temperature of 479.1, 475.6, and 480.3 °C is reported for PP-CNF-1, PP-CNF-2, and PP-CNF-3, respectively (Figure 10a–c) [4,34].

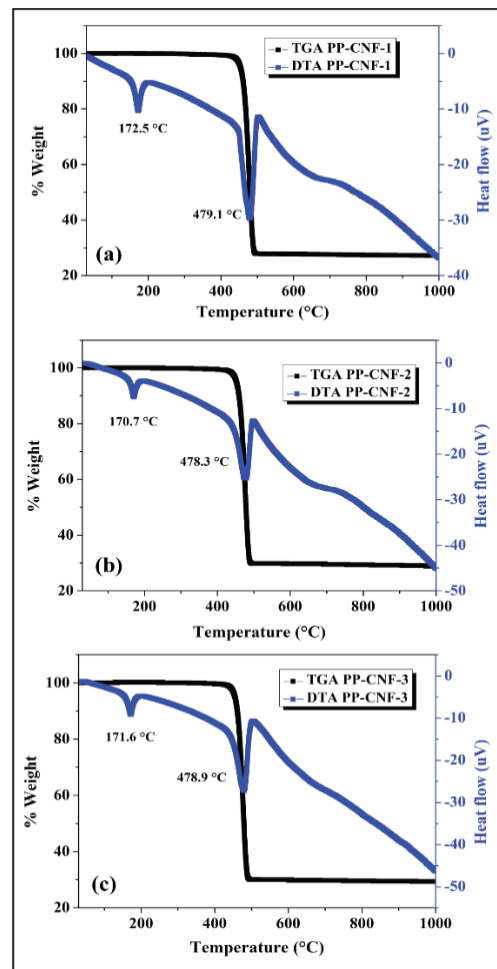


**Figure 10.** TGA and DTA curve of (a) PP-CNF-1, (b) PP-CNF-2 and (c) PP-CNF-3 nanocomposite.

### 3.4. FTIR Analysis of PP-CNF Nanocomposite

The chemical interaction between PP and CNF and the recycling effect on functionalities of PP are studied by FTIR (Figure 11). All the specimens are characterized in air and CNF background to see the interaction between CNF and PP. FTIR of CNF is done by extracting CNF from nanocomposites (by removing all the polymer), as shown in Figure 11a.

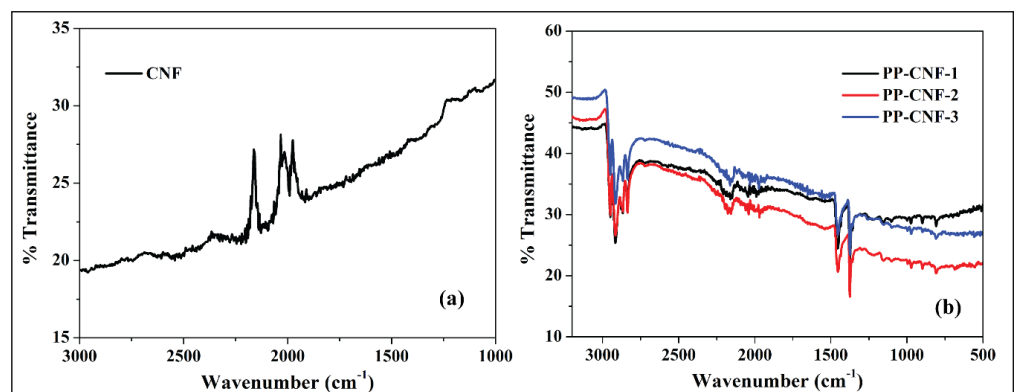


**Figure 11.** (a) FTIR spectra of CNF nanocomposites (b) FTIR spectra of PP-CNF nanocomposites.

Figure 11b shows the FTIR spectra of recycled PP nanocomposite in air background deduction. Figure 11a shows that there are no significant N and O functionalization peaks

on the CNF and peaks observed in Figure 11a designated to  $sp^2$  C and  $sp^3$  C in the form of C-C, C=C, and C-H of CNF. In Figure 11b, the symmetric bending vibration mode of  $-CH_3$  group of PP can be seen at  $1375\text{ cm}^{-1}$ , while the peaks at  $1455$ ,  $2838$ , and  $2917\text{ cm}^{-1}$  are attributed to  $-CH_2-$  symmetric bending,  $-CH_2-$  symmetric stretching, and  $-CH_2-$  asymmetric stretching of PP polymer, respectively [35,36]. It is observed that there is no significant difference in the peak intensity of the PP functional group registered due to the recycling of CNF (Figure 11b). It indicates no chemical change in the linkage between PP and CNF. Hence, the lowering of mechanical properties after every recycling result from intrinsic chemical behavior changes in PP and the aspect ratio of CNF, which affects the interfacial interaction behavior of nanocomposites.

#### 4. Conclusions

Recycling plastic material is a very crucial step for sustainable material development. Recycling plastic material caused significant property changes in the material. In this study, CNF showed an essential role in maintaining the mechanical and thermal properties of recycled PP nanocomposite. Using extruder and injection molding techniques, PP-CNF nanocomposite has been recycled twice, and change in mechanical properties have been studied. It is found that with the recycling of nanocomposite, 12 and 14% lowering of bending and tensile modulus of PP-CNF is reported. The decrement in mechanical properties is due to the recycling that weakens the interfacial bond between CNF and PP. The lowering of interfacial interaction has been studied using SEM, stress-controlled Rheometer, DSC, and XRD technique that showed the lowering of the aspect ratio of CNF and increments in crystallinity of PP after recycling, which resulted in changes in interfacial bonding. In addition, the thermal degradation temperature and melting temperature of PP-CNF nanocomposites do not significantly affect after recycling. In the present study, it should be pointed out that recycled PP-CNF nanocomposite can be applied as automotive parts because of low change in mechanical and thermal properties, and it can be utilized as a sustainable material for other structural applications.

**Author Contributions:** A.K.P.: Conceptualization, Methodology, Investigation, Writing—original draft, Visualization. T.Y.: Resources, Methodology, Writing—review and editing, Supervision. All authors have read and agreed to the published version of the manuscript.

**Funding:** This research received no external funding.

**Institutional Review Board Statement:** Not applicable.

**Informed Consent Statement:** Not applicable.

**Data Availability Statement:** Data is available on request from the authors.

**Acknowledgments:** The authors are thankful to ALMEDIO INC. for supplying the PP specimens.

**Conflicts of Interest:** The authors declare that they have no known competing financial interest or personal relationships that could have appeared to influence the work reported in this paper.

#### References

1. Jung, B.N.; Jung, H.W.; Kang, D.; Kim, G.H.; Shim, J.K. Synergistic Effect of Cellulose Nanofiber and Nanoclay as Distributed Phase in a Polypropylene Based Nanocomposite System. *Polymers* **2020**, *12*, 2399. [[CrossRef](#)] [[PubMed](#)]
2. Lebreton, L.; Andrady, A. Future scenarios of global plastic waste generation and disposal. *Palgrave Commun.* **2019**, *5*, 6. [[CrossRef](#)]
3. Lopez, G.; Artetxe, M.; Amutio, M.; Bilbao, J.; Olazar, M. Thermochemical routes for the valorization of waste polyolefinic plastics to produce fuels and chemicals. A review. *Renew. Sustain. Energy Rev.* **2017**, *73*, 346–368. [[CrossRef](#)]
4. Pathak, A.K.; Zhou, Y.; Lecointre, L.; Yokozeki, T. Polypropylene nanocomposites with high-loading conductive carbon nano-reinforcements for multifunctional applications. *Appl. Nanosci.* **2021**, *11*, 493–503. [[CrossRef](#)]
5. Lazim, N.H.; Samat, N. The influence of irradiated recycled polypropylene compatibilizer on the impact fracture behavior of recycled polypropylene/microcrystalline cellulose composites. *Polym. Compos.* **2019**, *40*, E24–E34. [[CrossRef](#)]
6. Tapper, R.J.; Longana, M.L.; Yu, H.; Hamerton, I.; Potter, K.D. Development of a closed-loop recycling process for discontinuous carbon fibre polypropylene composites. *Compos. Part B Eng.* **2018**, *146*, 222–231. [[CrossRef](#)]

7. Lopez, G.; Artetxe, M.; Amutio, M.; Alvarez, J.; Bilbao, J.; Olazar, M. Recent advances in the gasification of waste plastics. A critical overview. *Renew. Sustain. Energy Rev.* **2018**, *82*, 576–596. [[CrossRef](#)]
8. Li, Y.; Jia, S.; Du, S.; Wang, Y.; Lv, L.; Zhang, J. Improved properties of recycled polypropylene by introducing the long chain branched structure through reactive extrusion. *Waste Manag.* **2018**, *76*, 172–179. [[CrossRef](#)]
9. Chen, Y.; Wu, Z.; Fan, Q.; Yang, S.; Song, E.; Zhang, Q. Great toughness reinforcement of isotactic polypropylene/elastomer blends with quasi-cocontinuous phase morphology by traces of  $\beta$ -nucleating agents and carbon nanotubes. *Compos. Sci. Technol.* **2018**, *167*, 277–284. [[CrossRef](#)]
10. Lin, T.A.; Lin, J.-H.; Bao, L. Polypropylene/thermoplastic polyurethane blends: Mechanical characterizations, recyclability and sustainable development of thermoplastic materials. *J. Mater. Res. Technol.* **2020**, *9*, 5304–5312. [[CrossRef](#)]
11. Chen, T.; Zhang, J. Compatibilization of acrylonitrile-butadiene-styrene terpolymer/poly(ethylene glycol-co-1,4-cyclohexanedimethanol terephthalate) blend: Effect on morphology, interface, mechanical properties and hydrophilicity. *Appl. Surf. Sci.* **2018**, *437*, 62–69. [[CrossRef](#)]
12. Zaghoul, M.M.Y.; Mohamed, Y.S.; El-Gamal, H. Fatigue and tensile behaviors of fiber-reinforced thermosetting composites embedded with nanoparticles. *J. Compos. Mater.* **2019**, *53*, 709–718. [[CrossRef](#)]
13. Zaghoul, M.M.Y.; Zaghoul, M.Y.M.; Zaghoul, M.M.Y. Experimental and modeling analysis of mechanical-electrical behaviors of polypropylene composites filled with graphite and MWCNT fillers. *Polym. Test.* **2017**, *63*, 467–474. [[CrossRef](#)]
14. Zaghoul, M.Y.M.; Zaghoul, M.M.Y.; Zaghoul, M.M.Y. Developments in polyester composite materials—An in-depth review on natural fibres and nano fillers. *Compos. Struct.* **2021**, *278*, 114698. [[CrossRef](#)]
15. Zaghoul, M.M.Y.M. Mechanical properties of linear low-density polyethylene fire-retarded with melamine polyphosphate. *J. Appl. Polym. Sci.* **2018**, *135*, 46770. [[CrossRef](#)]
16. El-Fattah, A.A.; EL Demerdash, A.G.M.; Sadik, W.A.A.; Bedir, A. The effect of sugarcane bagasse fiber on the properties of recycled high density polyethylene. *J. Compos. Mater.* **2015**, *49*, 3251–3262. [[CrossRef](#)]
17. Lila, M.K.; Singhal, A.; Banwait, S.S.; Singh, I. A recyclability study of bagasse fiber reinforced polypropylene composites. *Polym. Degrad. Stab.* **2018**, *152*, 272–279. [[CrossRef](#)]
18. Corradini, E.; Ito, E.N.; Marconcini, J.M.; Rios, C.T.; Agnelli, J.A.; Mattoso, L.H. Interfacial behavior of composites of recycled poly(ethylene terephthalate) and sugarcane bagasse fiber. *Polym. Test.* **2009**, *28*, 183–187. [[CrossRef](#)]
19. Bourmaud, A.; Baley, C. Investigations on the recycling of hemp and sisal fibre reinforced polypropylene composites. *Polym. Degrad. Stab.* **2007**, *92*, 1034–1045. [[CrossRef](#)]
20. Chatterjee, A.; Deopura, B.L. Thermal stability of polypropylene/carbon nanofiber composite. *J. Appl. Polym. Sci.* **2006**, *100*, 3574–3578. [[CrossRef](#)]
21. Bannov, A.G.; Popov, M.V.; Kurmashov, P.B. Thermal analysis of carbon nanomaterials: Advantages and problems of interpretation. *J. Therm. Anal. Calorim.* **2020**, *142*, 349–370. [[CrossRef](#)]
22. Aurrekoetxea, J.; Sarrionandia, M.A.; Urrutibeascoa, I.; Maspoch, M.L. Effects of recycling on the microstructure and the mechanical properties of isotactic polypropylene. *J. Mater. Sci.* **2001**, *36*, 2607–2613. [[CrossRef](#)]
23. van der Lee, M.K.; van Dillen, A.J.; Geus, J.W.; de Jong, K.P.; Bitter, J.H. Catalytic growth of macroscopic carbon nanofiber bodies with high bulk density and high mechanical strength. *Carbon* **2006**, *44*, 629–637. [[CrossRef](#)]
24. Novais, R.; Covas, J.; Paiva, M. The effect of flow type and chemical functionalization on the dispersion of carbon nanofiber agglomerates in polypropylene. *Compos. Part A Appl. Sci. Manuf.* **2012**, *43*, 833–841. [[CrossRef](#)]
25. Pathak, A.K.; Dhakate, S.R. Carbon Nanomaterial-Carbon Fiber Hybrid Composite for Lightweight Structural Composites in the Aerospace Industry: Synthesis, Processing, and Properties. In *Advanced Composites in Aerospace Engineering Applications*; Springer: Berlin/Heidelberg, Germany, 2022; pp. 445–470.
26. Iwamoto, S.; Lee, S.-H.; Endo, T. Relationship between aspect ratio and suspension viscosity of wood cellulose nanofibers. *Polym. J.* **2014**, *46*, 73–76. [[CrossRef](#)]
27. Chen, X.; Wei, S.; Yadav, A.; Patil, R.; Zhu, J.; Ximenes, R.; Sun, L.; Guo, Z. Poly (propylene)/carbon nanofiber nanocomposites: Ex situ solvent-assisted preparation and analysis of electrical and electronic properties. *Macromol. Mater. Eng.* **2011**, *296*, 434–443. [[CrossRef](#)]
28. Aldica, G.V.; Ciurea, M.L.; Chipara, D.M.; Lepadatu, A.M.; Lozano, K.; Stavarache, I.; Popa, S.; Chipara, M. Isotactic polypropylene-vapor grown carbon nanofibers composites: Electrical properties. *J. Appl. Polym.* **2017**, *134*, 45297. [[CrossRef](#)]
29. Zhang, J.; Panwar, A.; Bello, D.; Jozokos, T.; Isaacs, J.A.; Barry, C.; Mead, J. The effects of recycling on the properties of carbon nanotube-filled polypropylene composites and worker exposures. *Environ. Sci. Nano* **2016**, *3*, 409–417. [[CrossRef](#)]
30. Jyoti, J.; Dhakate, S.; Singh, B.P. Phase transition and anomalous rheological properties of graphene oxide-carbon nanotube acrylonitrile butadiene styrene hybrid composites. *Compos. Part B Eng.* **2018**, *154*, 337–350. [[CrossRef](#)]
31. Jyoti, J.; Singh, B.P.; Rajput, S.; Singh, V.N.; Dhakate, S.R. Detailed dynamic rheological studies of multiwall carbon nanotube-reinforced acrylonitrile butadiene styrene composite. *J. Mater. Sci.* **2016**, *51*, 2643–2652. [[CrossRef](#)]
32. Fujii, Y.; Nishikawa, R.; Phulkerd, P.; Yamaguchi, M. Modifying the rheological properties of polypropylene under elongational flow by adding polyethylene. *J. Rheol.* **2019**, *63*, 11–18. [[CrossRef](#)]
33. Solomon, M.J.; Almusallam, A.S.; Seefeldt, K.F.; Somwangthanaroj, A.A.; Varadan, P. Rheology of Polypropylene/Clay Hybrid Materials. *Macromolecules* **2001**, *34*, 1864–1872. [[CrossRef](#)]

34. Ren, Y.; Wang, Y.; Wang, L.; Liu, T. Evaluation of intumescent fire retardants and synergistic agents for use in wood flour/recycled polypropylene composites. *Constr. Build. Mater.* **2015**, *76*, 273–278. [[CrossRef](#)]
35. Stoian, S.A.; Gabor, A.R.; Albu, A.-M.; Nicolae, C.A.; Raditoiu, V.; Panaitescu, D.M. Recycled polypropylene with improved thermal stability and melt processability. *J. Therm. Anal.* **2019**, *138*, 2469–2480. [[CrossRef](#)]
36. Yin, S.; Tuladhar, R.; Shanks, R.; Collister, T.; Combe, M.; Jacob, M.; Tian, M.; Sivakugan, N. Fiber preparation and mechanical properties of recycled polypropylene for reinforcing concrete. *J. Appl. Polym. Sci.* **2015**, *132*, 41866. [[CrossRef](#)]